# Deterioration of a compacted soil due to suction loss and desiccation cracking

Ashutosh Kumar[1] Arash Azizi[2*] and David G. Toll[3]

[1]Assistant Professor, School of Engineering, IIT Mandi, Mandi, Himachal Pradesh, 175005, India. Email: ashutosh@iitmandi.ac.in

[2*]Lecturer, School of Environment Geography and Geosciences, University of Portsmouth, Portsmouth, PO1 3QL, United Kingdom. Email: arash.azizi@port.ac.uk

[3]Professor, Department of Engineering, Durham University, Durham, DH1 3LE, United Kingdom. Email: d.g.toll@durham.ac.uk

*Corresponding author:

ABSTRACT

This paper presents the results of laboratory testing of a clayey soil taken from a road subgrade in Tanzania. The results revealed a reduction in the soil water retention capacity, accompanied by shifts in the water retention curves with successive cycles. These changes affected the soil response to shear loading, resulting in decreased shear strength and stiffness with hydraulic cycles. While the soil experienced suction losses due to desiccation cracks and hysteresis effects, these suction variations alone could not account for the observed changes in shear strength, implying that the development of desiccation cracks contributed to reduced strength and stiffness. The results showed that the degradation effect of crack development on the shear strength and elastic modulus of the soil during hydraulic cycles could be justified using a macroscopic degree of saturation, i.e. the degree of saturation of large pores external

to the aggregates, through a microstructural-based effective stress approach. This allowed the increase in the large pores resulting from crack development to be accounted for and hence the successive reductions in shear strength and stiffness with drying-wetting cycles. These deterioration effects need to be considered for design of geotechnical infrastructure to ensure stability, and resilience of infrastructure over time.

Keywords: suction; drying and wetting; shear strength; stiffness

## 1.0 INTRODUCTION

Compacted soils that usually form the foundation bed of linear infrastructure such as roads and railways can remain unsaturated during their service life, particularly in tropical climatic regions, and are often exposed to atmospheric interactions. These soils undergo drying and wetting due to environmental loading brought about by weather events. This hydrological change causes many geotechnical problems such as shrinkage settlement due to extreme drying and shear strength failure due to intense rainfall, leading to premature loss of serviceability of infrastructure and causing huge distress to the economy (Ng and Pang 2000; Tang et al. 2011; Goh et al. 2014; Toll 2015; Mendes and Toll 2016; Stirling et al. 2021; Xu et al. 2021). The response of unsaturated soils to hydro-mechanical loading is dependent on soil water retention properties, i.e. soil suction and water content (Toll 1990; Wheeler 1996; Gallipoli et al. 2003; Azizi et al. 2023a). The drying and wetting cycles can alter the soil fabric associated with volumetric expansion – contraction (Lloret et al. 2003; Airò Farulla et al. 2010; Azizi et al. 2020b) and crack development (Albrecht and Benson 2001; Yu et al. 2021; Xu et al. 2022). These changes in the microstructure and macrostructure of soils influence the pore pressure regime, water distribution, and the development of suction, which ultimately govern the soil strength in unsaturated conditions. Therefore, understanding the performance of linear infrastructure requires assessment of the effects of drying and wetting cycles on water retention properties and mechanical characteristics of compacted soils forming their substructure.

Soil's capacity to develop the suction-induced strength is dependent on the hydraulic history while soil water retention capacity evolves during drying and wetting cycles leading to subsequent changes in the mechanical behaviour of unsaturated soils. Several researchers (e.g. Fredlund and Xing 1994; Goh et al. 2014; Azizi et al. 2020b; Mu et al. 2020) reported that major hysteresis and evolution of the soil water retention behaviour occurs during the initial cycles of drying-wetting while these alterations become negligible in the following cycles due to the soil fabric reaching a stable state. Besides this, desiccation cracking is commonly observed in soils containing an appreciable proportion of fines while the extent of cracking is dependent on the water content and the evolved suction associated with drying-wetting cycles (Fredlund and Rahardjo 1993; Zuo et al. 2016; Albrecht and Benson 2001). It has been pointed out that subsequent drying and wetting under field environmental conditions are the main triggering factors for the development of cracks that can lead to the reduced strength of the soil matrix (Hen-Jones et al. 2017; Yu et al. 2021). Azizi et al. (2018; 2020b) and Stirling et al. (2021) tested clayey soils and reported the development of microcracks within the soil due to alternate drying and wetting cycles results in micro-structural changes in terms of the pore size distribution, which eventually affect the hydro-mechanical properties of soils. Although the influence of soil water retention properties and crack development on the soil strength have been discussed, the dominant mechanism causing the strength degradation of soils under hydraulic cycles considering the combined effects of evolving suction and desiccation cracking have not been explicitly addressed.

This study provides evidence of the deterioration effects of drying-wetting cycles on both the hydraulic and the mechanical behaviours of a compacted soil, providing insights into the interrelation between these two aspects. First, the compaction characteristics of soil samples are discussed when the samples were subjected to various numbers of drying and wetting cycles. Next, the water retention response in terms of the soil water retention curve and the shrinkage curve, and the evolution of suction with water content of dried and wetted samples are considered. Thereafter, constant water content triaxial tests were performed on as-compacted, dried and wetted samples. The obtained experimental results were examined to establish a link between wetting and drying processes and the changes in soil water retention capacity, shear strength and stiffness.

## 2.0 MATERIAL AND SAMPLE PREPARATION

Soil samples were recovered from the subgrade layer of a low-volume road in the Lawate region located in the North-East part of Tanzania. Most low volume roads in the rural area of Tanzania are unpaved or sealed with poor surfacing. Therefore, these roads are exposed to atmosphere interactions and can deteriorate due to changing weather conditions while requiring frequent maintenance over their service life (Chinowsky et al. 2013). The material recovered was a clayey soil containing 43% clay, 44% silt, and 13% sand. A significant clay content suggests that the subgrade material can be highly susceptible to fluctuations in the moisture content induced by seasonal variations. The liquid limit, plasticity limit and specific gravity (BS 1377-2,

1990) of the air-dried natural soil are 51.4%, 34.9% and 2.66. The material was oven-dried for 24h, then mechanically ground prior to sample preparation. The Atterberg limits of the oven-dried samples were also measured, and the liquid limit was found to be 47.2% and the plastic limit 32.5%. This showed that oven-drying did not significantly affect the consistency limits of the tested soil. The optimum water content of 24% and the maximum dry density of 1.62 Mg/m$^3$ were obtained by standard Proctor compaction following BS 1377- 4 (1990).

The oven-dried soil powder was mixed with distilled water equivalent to the optimum water content and sealed in a plastic bag for 24h for water homogenisation. Next the wet soil was statically compacted in 4 layers to form cylindrical samples of 38 mm in diameter and 76 mm in height where a dry density of 1.54 ± 0.02 Mg/m$^3$ was achieved. A cross grooving was made at the soil surface after the compression of each layer to ensure a good contact between layers and prepare a uniform sample. The rate of application of the axial displacement during compaction was maintained very low (0.15 mm/min) to avoid the development of any excess pore-water pressure that might affect the sample homogeneity. The sample was removed from the cylindrical brass mould by using a rate controlled mechanised sample extruder having a piston with a diameter of 37 mm. The compacted samples were then sealed in plastic bags while their weight and dimensions were carefully recorded at certain time intervals. No volume change was recorded after about 24h while the weight of the samples remained constant. Table 1 gives the details of the tested samples.

## 3.0 TESTING PROCEDURE

### *3.1. Drying and wetting*

The compacted samples were subjected to alternate cycles of drying and wetting (up to 6 cycles) to mimic the effect of repeated evaporation and precipitation under field conditions. As shown in Figure 1a, the drying path was imposed by air-drying at a constant temperature of 20°C (±0.5°C) and a relative humidity of 39% in a laboratory environment (to achieve a suction $s$ ~ 132 MPa). The water content was decreased until the attainment of a residual water content condition for each step of the drying process. The wetting path was imposed by placing the sample in a closed chamber at a high relative humidity (close to 100%) as shown in Figure 1b (following the approach explained in Kumar et al. 2022).

This process of vapour absorption, with a small amount of capillary absorption from condensation, should lead to homogeneous distribution of water across the sample. However, samples were then sealed in a plastic bag for at least 48h to ensure water homogenisation. The rate of evaporation during drying and water absorption during wetting remained consistent across all samples. The duration of wetting or drying process varied depending on the initial water content of the samples, as samples with different water content possess varying permeability values. The wetting process varied between 5 hours to 150 hours. In the case of a fully air-dried sample, it took about 105 hours to wet up to a water content of 15% and 150 hours to attain a water content of 24%.

The weight and dimensions of the sample were frequently measured (an average time interval of 4 hours) during drying and wetting using a digital balance (with a precision of 0.0001g) and a calliper (with a precision of 0.01 mm), respectively. As samples maintained a uniform cylindrical shape, volume measurements were achievable by measuring the dimensions of the samples. The diameter of the samples was measured at three locations including mid and end portions while the height of the sample was measured at two locations in diametrically opposite directions. The samples were relatively stiff therefore no disturbance was observed during this process. After each cycle of drying and wetting, the sample was kept in a plastic bag for at least 48h for water homogenisation. Similar methods for volume measurements for water retention testing were adopted by Azizi et al. (2020a), Azizi et al. (2023), Dias et al. (2023) and Li et al. (2023).

As shown in Table 1, the samples used for testing had different water contents as they were preserved and collected from distinct stages along the imposed drying or wetting paths, ranging from the 1$^{st}$ to the 6$^{th}$ hydraulic cycle.

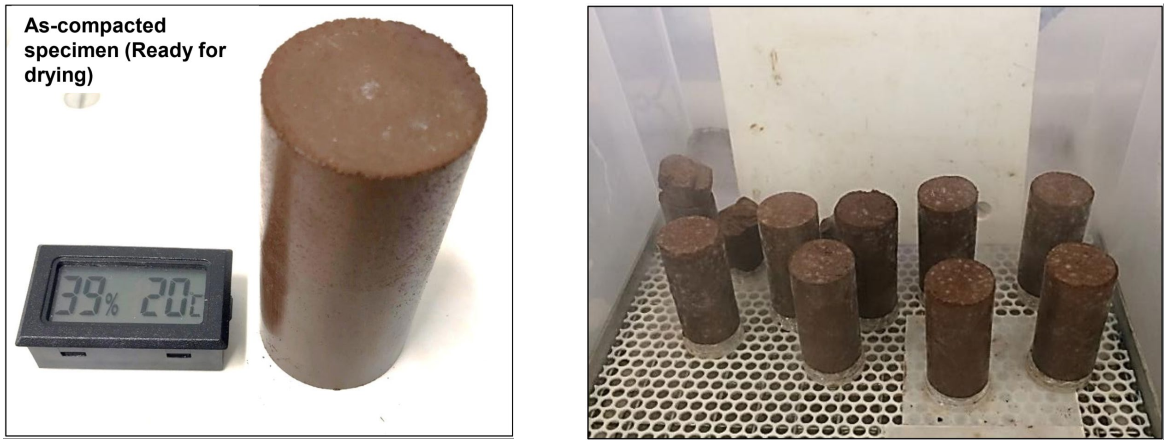


(a) (b)

Fig 1. Applying drying and wetting to the compacted sample
(a) air drying (b) wetting in a chamber

Figure 2a shows the variation of the water content for one of the samples under 6 drying and wetting cycles. “As” indicates the as-compacted state, and “D” and “W” indicate the drying and wetting cycles from 1$^{st}$ to 6$^{th}$ cycle. The drying paths were continued until the attainment of a stable water content at a fully air-dried state ($w_{avg}$ = 1.5%) and the wetting paths were imposed until the water content reached around the initial water content of the samples ($w_{avg}$ = 24%).

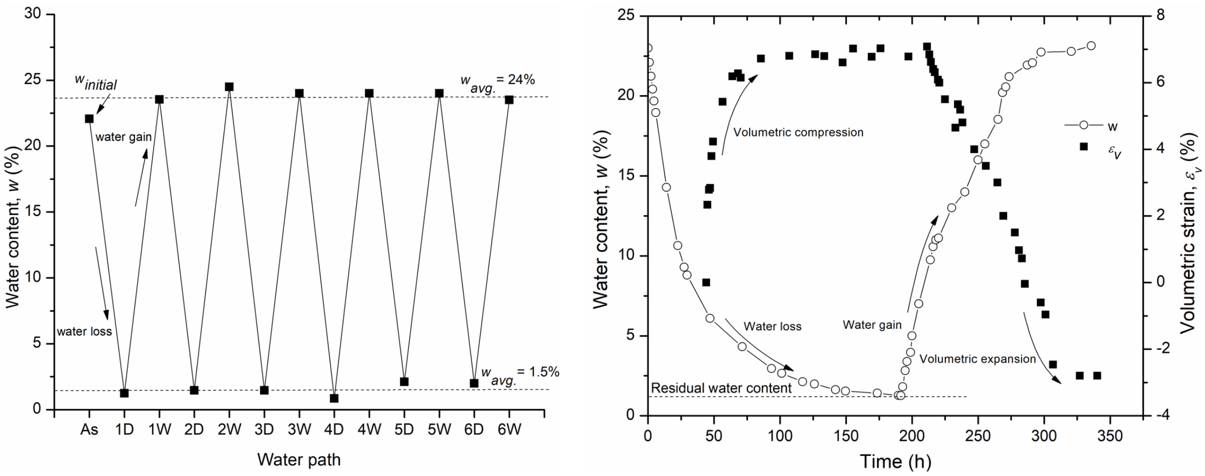


(a) (b)

Fig 2. (a) Variations of water content with wetting and drying paths (b) Volumetric strains along one cycle of drying and a wetting

Figure 2b shows the measured volumetric strain $\varepsilon_v$ and gravimetric water content $w$ with respect to the elapsed time during one cycle of drying and wetting. During the drying process, the contractive volumetric strain (positive) during shrinkage stabilised (within 75h) earlier than the variation of the water content that stabilised within 180h of air-drying. This is likely because the deformation took place primarily due to the fast surficial evaporation and diminished during the delayed central core drying. The measured volumetric expansion (negative volume strain) during wetting was more consistent with the rate of the increase in the water content as water condensation caused by a high relative humidity air around the soil sample increased the water content across the sample more homogeneously. The sample indicated irreversible volume changes exhibiting a contractive volumetric strain of +6.5% at the end of the 1$^{st}$ drying path and an expansive volumetric strain of -2.8% at the end of the 1$^{st}$ wetting path.

*3.2. Water retention testing*

Several samples were used for determination of the water retention properties (suction and water content) of the tested soil. These samples were taken at certain water content values along 1st, 3rd, and 6th cycle of drying or wetting paths. The suction was measured on a cut portion of the sample core using a dew point potentiameter (WP4C) with an accuracy of ±0.05 MPa from 0 to 5 MPa and 1% from 5 to 300 MPa (ASTM D6836, 2002; Meter 2018) while the water content was obtained by weight measurements. The suction considered in the analysis is total suction as measured by WP4C. Therefore, the individual effects of osmotic and matric suction were not specifically examined.

### *3.3. Triaxial testing*

The other samples were used for triaxial testing where the water drainage was closed during compression and shearing (constant water content condition). The shear behaviour of 26 samples at different water content levels along the drying and wetting paths was investigated at a constant confining pressure of 25 kPa which is a typical confining stress present at the subgrade layer of low-volume roads. An axial displacement rate of 0.063 mm/min was imposed during shearing. The water content and suction measurements were carried out using the core portion of the samples recovered immediately at the end of the triaxial tests. It was then assumed that the suction measured at the end of the test represents the suction level during shearing as a very low permeability of the tested soil reduces the rate of the water redistribution and suction equalisation within the samples.

## 4.0 RESULTS

### *4.1 Volumetric behaviour*

Figure 3 shows the hydraulic path applied and the volumetric strains of all samples measured after they were subjected to different numbers of drying and wetting cycles. The samples were taken at different water content values along the drying and wetting paths that lead to development of compressive (negative) or expansive (positive) volumetric strains, respectively. The samples showing small volumetric strains are those with the water content values close to the initial water content at the as-compacted state and the samples showing greater volumetric strains are those at drier or wetter states compared to their initial water content.

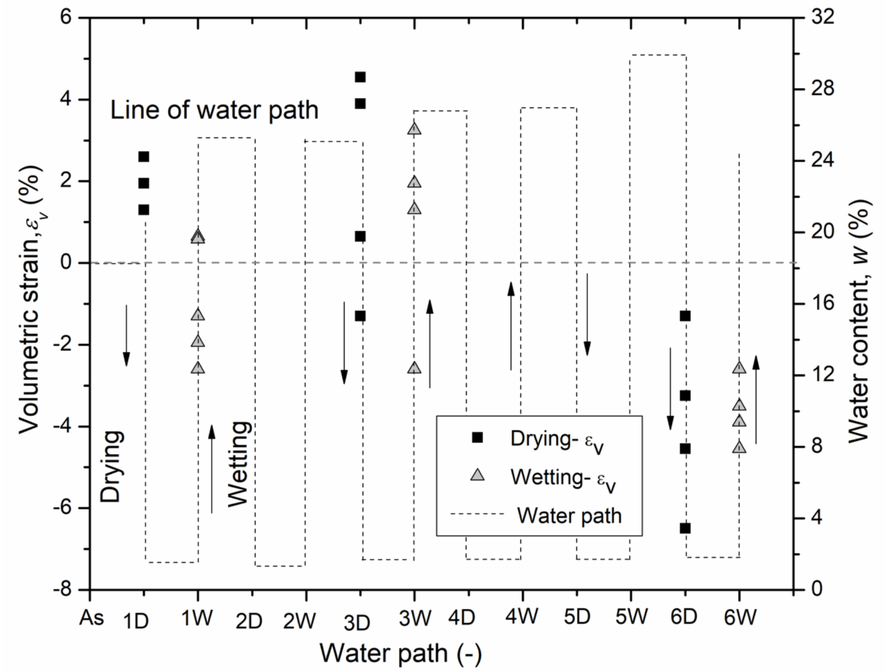


Fig 3. The volumetric strains measured along the applied hydraulic loading paths

For the samples subjected to one cycle, the volumetric strains showed that the dried samples (1D) experienced contractive volumetric strains while the wetted samples (1W) mostly exhibited expansive volumetric strains regardless of their water content levels. The volumetric strains showed a gradual increase from the 1st to the 3rd cycle, with a growing tendency for the samples to exhibit contractive strains. These irreversible volumetric strains developed during initial drying and wetting cycles are likely to be due to fabric rearrangement during suction changes or the development of micro-cracks within the aggregate structure of the samples as also discussed by Cui et al. (2002), Nowamooz and Masrouri (2009) and Azizi et al. (2020b).

However, the expansive volumetric strains further increased during the subsequent drying and wetting cycle, particularly noticeable in the samples exposed to 6 cycles of drying and wetting (6D/W). It can be observed that even the samples dried to the target water contents failed to recover any contractive strains during the shrinkage process. No visible cracks on the samples were observed during the initial drying-wetting cycles (after applying 1$^{st}$ and 3$^{rd}$ drying) as shown in Figures 4a and 4b. However, the micro-cracks developed during initial cycles occasionally became apparent surficial cracks after about 4 cycles of drying and wetting (see the surficial cracks on the body of the sample subjected to 6$^{th}$ drying as shown in Figure 4c).

It should be noted that the visible cracks on the sample likely developed during the drying process. This is mainly due to the shrinkage of the sample and the presence of the boundary condition on the sample body that developed non-homogenous stress state thereby producing tensile local stresses and cracking.

The presence of surficial cracks and internal discontinuities within the soil mass seemed to increase the tendency of the samples to exhibit expansive volumetric strains while reducing their inclination to develop contractive strains between the 3$^{rd}$ and 6$^{th}$ cycles. It is worth noting that the appearance of these cracks mostly occurred during 3$^{rd}$ and 5$^{th}$ cycles while no further crack development was detected during the subsequent cycle.

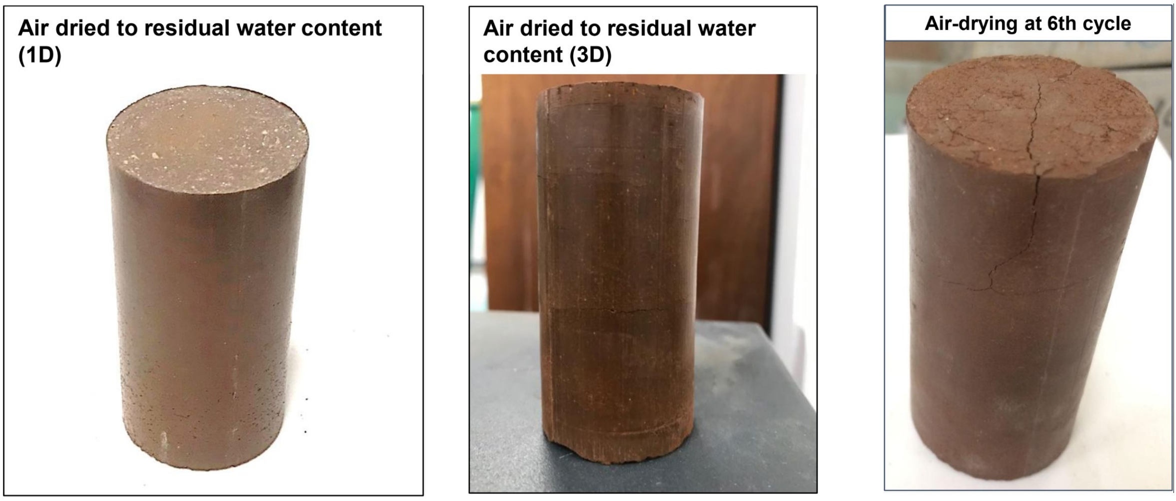


(a) (b) (c)

Fig 4. The condition of the dried samples (a) after applying 1st drying (b) after applying 3rd drying (c) after applying 6th drying

Figure 5 shows the compaction curve for the tested soil together with the water content and density state of all samples used for triaxial testing (after compaction and applying drying and wetting cycles) in terms of the dry density ($\rho_d$) and water content ($w$). This indicates how the state of the sample changes due to volumetric expansion-contraction when they were subjected to cycles of hydraulic loading. Although the samples were prepared at a constant dry density of about 1.54 Mg/m$^3$, the cycles of drying and wetting changed the dry densities of the compacted samples due to volumetric expansion and contraction brought about by adsorption and desorption of water as discussed earlier.

The dried samples lay close to the dry side of the compaction curve as their water contents decreased during drying, accompanied by an increase in suction (as indicated by the labels of the data points in Figure 5). The wetted samples lay close to the wet side of the compaction curve as their water contents increased during wetting, accompanied by a decrease in suction.

The samples subjected to one cycle (1$^{st}$ drying or wetting, 1D/W) showed transitions between the dry and wet sides of the optimum water content due to dying and wetting, following a trend within an area defined as Zone I as shown in Figure 5. The samples subjected to 3 drying-wetting cycles (3$^{rd}$ drying or wetting, 3D/W), showing greater volumetric contractions along the hydraulic paths, lay within the area defined as Zone II which had higher density values compared to Zone I, and samples subjected to 6 drying-wetting cycles (6$^{th}$ drying or wetting, 6D/W), showing increased volumetric expansions after 4 cycles, lay within Zone III which represented lower density compared to the other zones.

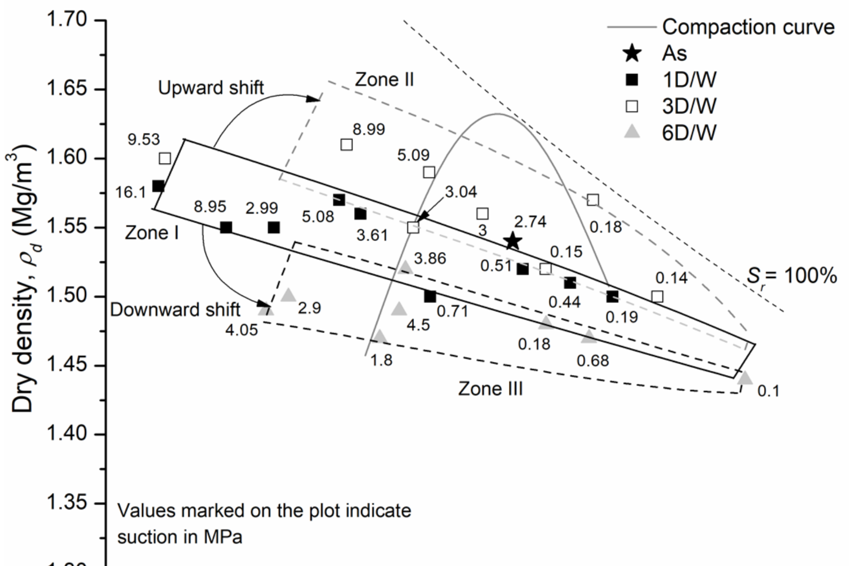


Fig 5. The compaction state of the as-compacted, dried and wetted samples

The results imply that the density and water retention state of the tested soil changes due to the fabric change and development of the cracks with drying and wetting cycles.

As a consequence, the density increases from 1st to 3rd cycle while it reduces when the soil is subjected to 6 cycles.

### *4.2 Water retention behaviour*

Figures 6 show the experimental water retention and shrinkage data for different cycles of drying and wetting and the curves fitted to experimental data generated by the van Genuchten (vG) model (van Genuchten, 1980). The least squares method of curve fitting was used to obtain the parameters of the vG model. The water retention experimental data indicated hysteretic water retention behaviour between the drying (Figure 6a) and wetting (Figure 6b) paths.

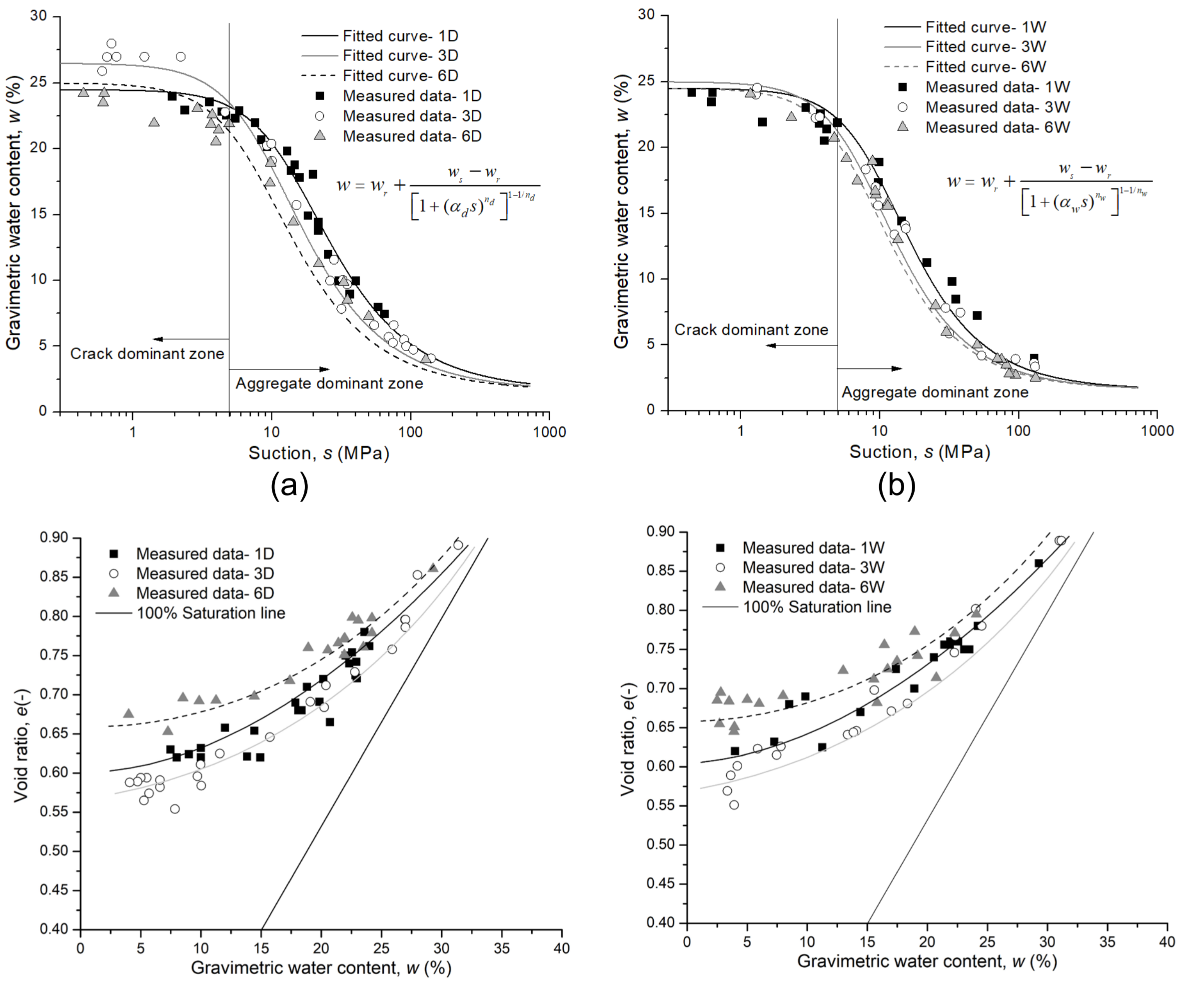

(c) (d)

Fig 6. The water retention experimental and modelling data (a) $w$ - $s$ along the drying path (b) $w$ - $s$ along the wetting path (c) $e$ - $w$ along the drying path (d) $e$ - $w$ along the wetting path

Two different water retention trends can be observed in both datasets along hydraulic cycles. The results indicated a progressive suction loss with drying-wetting cycles for suction levels $s$ > 4.5 MPa where the shift of the water retention curve to the lower suction levels was slightly more evident from 1D (or 1W) to 3D (or 3W) compared to the shift from 3D (or 3W) to 6D (or 6W).

For suction levels $s$ < 4.5 MPa, the trend was different, particularly for the drying paths (Figure 6a), where the water retention capacity increased from 1D to 3D as the water retention curve shifted upward. It then decreased from 3D to 6D associated with the downward movement of the curve. This can also be observed in terms of the saturated water content ($w_s$) where it increased (24.5 % to 26.5 %) from 1D to 3D followed by the decrease in the saturated water content (26.5 % to 25%) from 3D to 6D. Similar changes in the saturated water content can be seen during wetting cycles although they were not as evident as the drying cycles.

It can be pointed out that for $s$ > 4.5 MPa, the micropores within the clay aggregates would govern the evolution of the suction (Romero et al. 2011) and hence the soil water retention capacity reduces because of the decrease in the size of the aggregates or the breakage of the aggregates into smaller pieces due to progressive development of microcracks during drying-wetting cycles (Azizi et al. 2020b; Stirling et al. 2021). Also, it can be stated that the effect of hydraulic hysteresis reduces with an increase in the number of drying and wetting cycles (Wen et al 2021). This is mainly because the suction within the clay aggregates tended to stabilise with initial cycles and did not seem to be significantly affected by the surficial cracks with further cycles.

For $s$ < 4.5 MPa, the water retention behaviour would be governed by macropores where the saturated water content of the sample increased from 1$^{st}$ to 3$^{rd}$ cycles. This increase can be attributed to the volumetric expansion observed at the end of the 2$^{nd}$ wetting path which increased the pore space within the soil mass, facilitating further accumulation of water at low suction levels along the 3$^{rd}$ cycle. At these suction levels, the desiccation cracking observed on the surface of the sample subjected to 6 cycles also affected the water retention capacity. As these surficial cracks are of equivalent size to larger pores, the suction levels applied during wetting were not low enough to make these large pores retain water. This resulted in the reduction of the water retention capacity of the soil associated with the reduction in the saturated water content of samples subjected to 6 cycles compared to those subjected to 3 cycles.

Figure 6c shows the experimental shrinkage curve data for cycles of drying (Figure 6c) and wetting paths (Figure 6d). As the water content increases, all samples tend towards the saturation line. However, the position of the shrinkage curves varies among samples subjected to different cycles. Samples experiencing initial hydraulic loading cycles, from the 1$^{st}$ to the 3$^{rd}$ cycles, exhibit a reduction in void ratio, placing the shrinkage curve of 3D (or 3W) below that of 1D (or 1W). This is attributed to the accumulation of compressive volumetric strains during the initial cycles, as previously discussed with respect to the state of the samples shown in Figure 5. On the other hand, the shrinkage curves of the samples subjected to the 6$^{th}$ cycle lie above those of samples subjected to the 1$^{st}$ and 3$^{rd}$ cycles due to an increase in the void ratio resulting from soil volume expansion during subsequent cycles. This is evident in the increase of the void ratio values at the driest state, where the average void ratio rises from 0.57 to 0.67 from 3D to 6D samples. This pattern is primarily due to the reduced capacity of the soil to recover its contracted volume, due to the development of micro-cracks and visible surface cracks.

Figure 7 shows the suction loss ($\Delta s$) resulting from the well-known hysteretic characteristics of the soil water retention behaviour (Hillel 1998) where $\Delta s$ refers to the suction difference between the drying and wetting paths at the same water content level. The amount of $\Delta s$ increased with a decrease in the water content but decreased from 1$^{st}$ to 6$^{th}$ cycle, implying that the hysteresis evolved with hydraulic cycles. It is noticeable the reversal in the shape of the $\Delta s$ curves at high water contents for the 3$^{rd}$ and 6$^{th}$ cycle, that can be attributed to cracking. Besides $\Delta s$ caused by hysteresis, the suction loss from 1$^{st}$ to 6$^{th}$ cycle due to the shifts in either the drying or wetting curves is also shown in Figure 7, i.e. the difference between suctions at the 1$^{st}$ and 6$^{th}$ cycle (either the drying or wetting paths) at the same water content level. This latter suction loss was induced by the combined effects of fabric changes and crack development during hydraulic cycles which altered the water retention properties of the tested soil, leading to suction loss that is as significant as the hysteresis phenomenon. These reductions in soil water retention capacity and suction generation were also reported at a field scale, where smaller suctions were gradually developed within earth structures subjected to seasonal variation for the same change in soil water content (Stirling et al. 2021; Rouainia et al. 2021). Such changes contribute to the degradation of soil hydro-mechanical properties, resulting in the deterioration of earthworks made of compacted soils and an increase in failure rates of transportation infrastructure (Briggs et al. 2023).

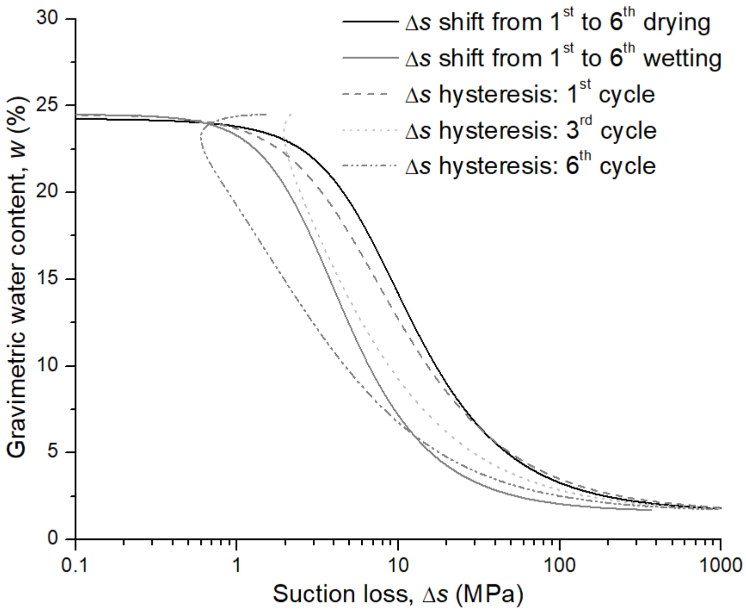


Fig 7. Suction loss due to hysteresis and shifts in the water retention capacity with drying and wetting cycles

Figures 8a and 8b show the experimental water retention data in terms of degree of saturation and suction for different cycles of drying and wetting and the curves predicted the vG model. Table 2 shows the values of the model parameters used to simulate the drying and wetting experimental data. The degree of saturation curves provide insights into how water occupies pore volume within the soil matrix, making it more reliable for assessing and predicting soil water retention relationships under varying void ratio (Pasha et al. 2016). However, when water exists in the absorptive regime, the suction is largely controlled by water content (Romero et al. 2011; Azizi et al. 2020b; Dias et al. 2023) and less influenced by density (or degree of saturation), as density is controlled by the presence of air-filled macro voids that do not influence suction. Nevertheless, in the capillary regime, at low suctions, the macro voids can become filled and thus affect the water retention behaviour.

Although full saturation was not achieved because the minimum suction reached at the end of wetting was not low enough to fully saturate the large pores and the cracks that formed during drying and wetting, the shifts observed in terms of gravimetric water content are also evident in Figures 8a and 8b where the water retention curves are shown in terms of degree of saturation. These shifts indicate a reduction in water retention capacity with drying-wetting cycles that is not attributable to the influence of void ratio changes. For instance, from the 1st to the 3rd cycles, samples experienced a decrease in void ratio, as discussed earlier. It was expected that the water retention curves would shift towards higher suctions with an increase in the air entry value. However, in this study, the water retention curve shifts towards lower suction levels from 1D (or 1W) to 3D (3W), mainly due to microstructural changes taking place in the soil fabric that dictate the water retention behaviour rather than the overall macroscopic void ratio (Azizi et al. 2020b).

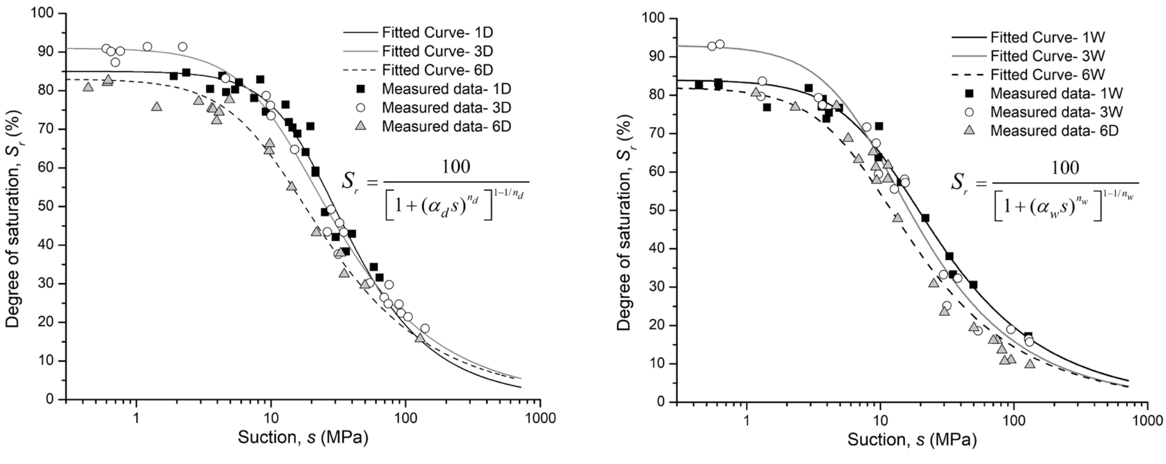


(a) (b)

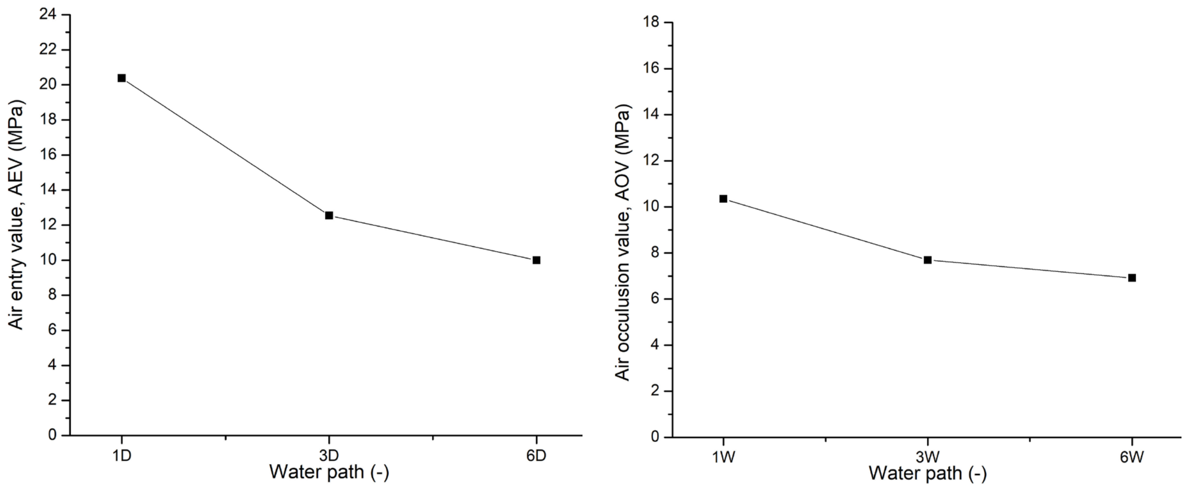


(c) (d)

Fig. 8. The water retention experimental and modelling data (a) $Sr$ - $s$ along the drying path (b) $Sr$ - $s$ along the wetting path (c) air entry value (d) air occlusion value

On the other hand, the samples subjected to 6 cycles, exhibiting an increase in void ratio, also exhibit shifts towards lower suction levels with a decrease in the air entry values. This trend can be explained by the impact of the void ratio, as crack development and volumetric expansion during further hydraulic cycles introduce more voids into the soil which lead to the increase in the void ratio and the decrease in the water retention capacity (Gallipoli et al. 2003; Tarantino 2009; Azizi et al. 2023b). The successive reduction in the air entry values, determined from water retention curves presented in terms of degree of saturation, from the 1st to the 3rd cycles, and then to the 6th cycles, can be observed in Figure 8c. A similar trend, with lesser variations, was observed for air occlusion values obtained along the drying and wetting cycles (Figure 8d).

*4.3 Shear strength behaviour*

Figure 9 shows the stress-strain behaviour of the dried and wetted samples during the 1st hydraulic cycle in terms of deviatoric stress $q$ and axial strain $\varepsilon_a$. Figure 9a shows that the peak deviatoric stress increased from 2.16 MPa to 4.82 MPa with the decrease in the water content from 20.6% to 16.2% during drying. Consequently, as the water content of the wetted samples increased from 17.6% to 22.1% during wetting, the peak deviatoric stress decreased from 2.66 MPa to 0.72 MPa as shown in Figure 9b. At the same water content levels, the wetted samples showed lower strength values when compared to the dried samples. Similar trends were also observed in samples subjected to 3 and 6 drying and wetting cycles.

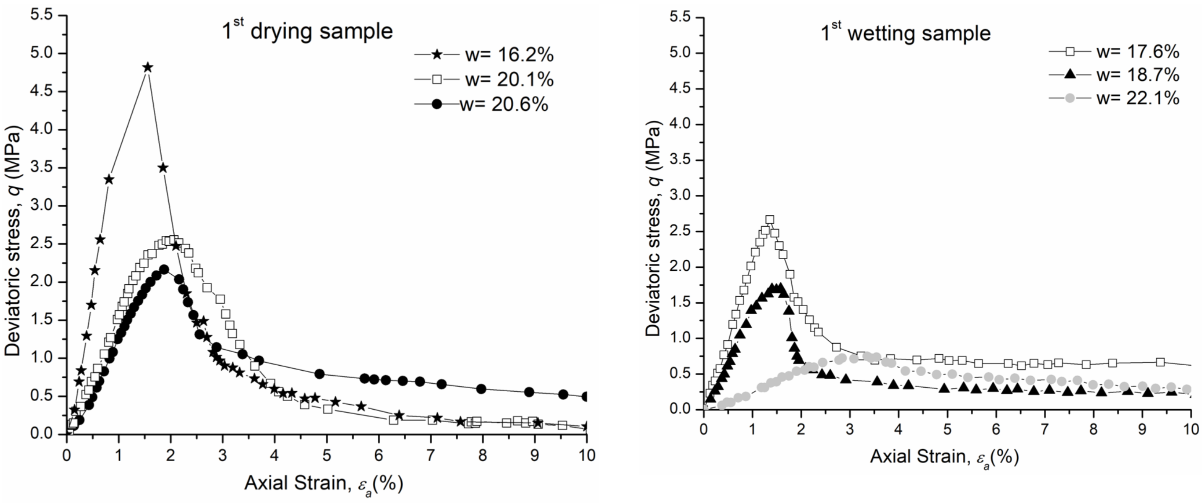


(a) (b)

Fig 9. The deviatoric stress and axial strain during the 1st cycle
(a) dried samples (1D) (b) wetted samples (1W)

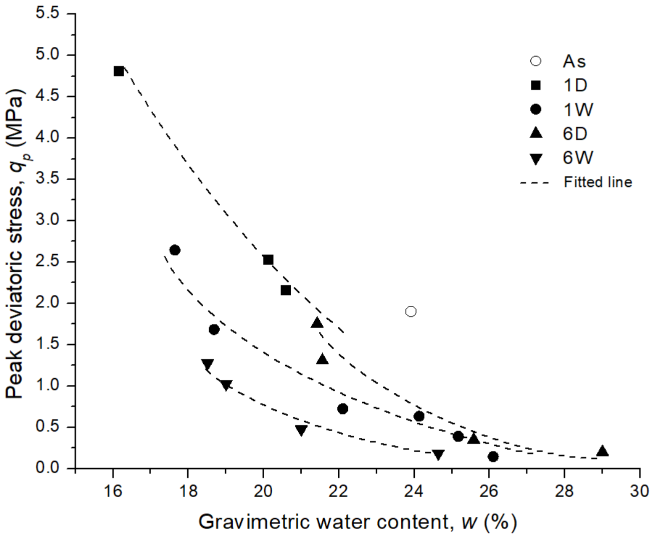

Fig 10. The peak deviatoric stress and water content for all sample

Figure 10 shows the variation of the peak deviatoric stress $q_p$ with respect to water content $w$ for the samples subjected to the 1st and 6th cycles including 1D, 1W, 6D and 6W. The results indicate that $q_p$ was not only dependent on the water content of the samples but also on the hydraulic history which affected how the suction evolved within the soil as will be discussed in the following. The peak strength reduced from the drying to the wetting paths, i.e. from 1D to 1W and from 6D to 6W. Also, $q_p$ decreased from the 1st cycle to the 6th cycle, i.e. from 1D to 6D and from 1W to 6W.

Figure 11a shows the stress-strain behaviour of an as-compacted sample (As) with $w$ = 23.9% and samples dried to water contents of 20.6% and 16.2% during the 1st cycle (1D) and 16.3% during the 3rd cycle (3D). The peak deviatoric stress of the As and 1D samples increased from 1.91 MPa to 4.82 MPa with an increase in the suction ($s$) from 2.74 MPa to 16.1 MPa during drying. The soil became stiffer and brittle with an increase in $s$ due to the bonding effect brought about by suction increments. However, the dried sample during the 3rd cycle (3D), despite having a similar water content to the driest 1D sample ($w$ = 16.2-16.3%), exhibited a reduction in peak stress from 4.82 MPa to 3.42 MPa. This decrease can be attributed to the loss of suction from 1D to 3D, where the suction decreased from 16.1 MPa to 9.53 MPa, despite similar water content levels. This suction loss is consistent with the shift of the drying water retention curves with successive cycles observed for a suction range greater than 4.5 MPa as discussed earlier. Similar response of strength degradation due to the development of desiccation cracks were reported by Tang et al. (2020) for high-plasticity clay.

Figure 11b shows $q$-$\varepsilon_a$ behaviour of samples subjected to 1st drying (1D), 1st wetting (1W), 3rd drying (3D) and 6th drying (6D) cycles having water contents of 20.1%, 18.7%, 21.7% and 21.6%, respectively. Comparing 1D to 1W, the wetting phase reduced the soil suction from 5.08 MPa to 2.99 MPa due to the hysteresis of the water retention behaviour, leading to the reduction of the peak strength from 2.6 MPa to 1.7 MPa. On the other hand, the dried sample subjected to 3 cycles (3D) exhibited a peak strength similar to 1W as the suction level of both samples were about 3 MPa.

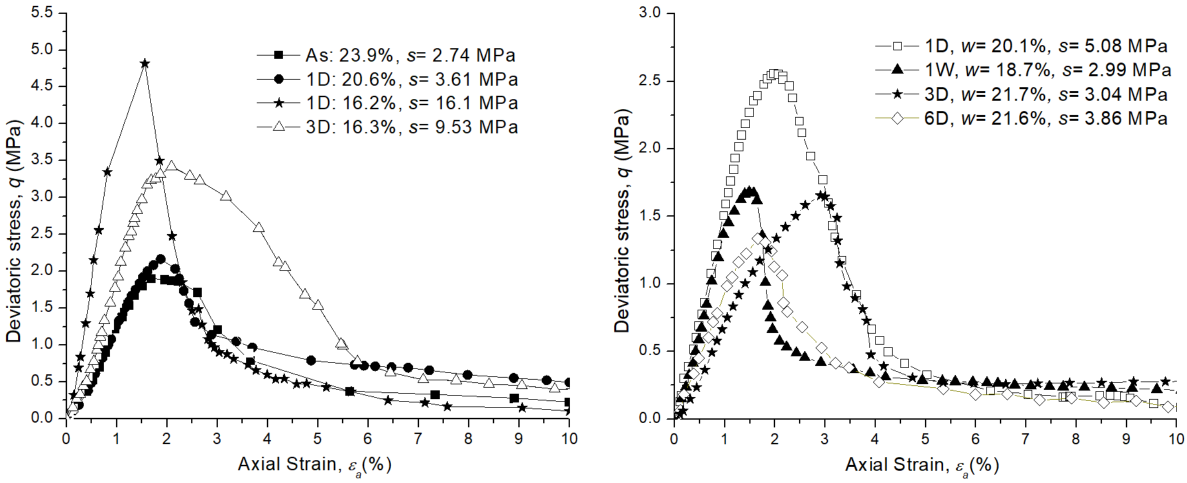


(a) (b)

Fig 11. The deviatoric stress and axial strain for (a) as-compacted, 1D and 3D samples (b) 1D 1W, 3D and 6D samples

The results discussed above suggest the shear strength of the soil depends on the suction levels within the samples which undergo changes during the drying and wetting processes. These changes lead to suction losses because of the hysteresis observed between the drying and wetting paths, as well as the shifts in the water retention capacity with successive cycles. However, it is noteworthy that the samples subjected to 6 cycles showed lower peak strength levels compared to those subjected to a lower number of cycles at the same suction levels. For example, as shown in

Figure 10b, 6D exhibited a lower peak deviatoric stress (1.41 MPa) despite having a higher suction level compared to 1W and 3D. This implies that the reduction in the strength observed in samples subjected to 6 cycles is not only attributable to the suction loss but also the development of micro-cracks as discussed in section 5.

*4.4 Stiffness behaviour*

Some researchers, e.g. Fredlund et al. (1975), Ng et al. (2009) and Lu and Kaya (2014), have noted that the stiffness properties of unsaturated soils depend on their suction level. However, the stress-strain relationships observed in some of the samples during shearing, shown in Figures 9 and 11, suggest that the stiffness of the tested soil may not be solely dependent on soil suction levels (or water content levels). For instance, in Figure 11b, the peak strengths of 3D and 1W having a similar suction (about 3 MPa) were found to be at the same level but they took place at different strains implying the stiffness of these two samples was different.

It has to be pointed out that the soil stiffness depends on both strain and suction levels. However, the above-mentioned observation on the stiffness was found to be consistent regardless of the strain level. As this study aimed to highlight the effect of hydraulic cycles on the evolution of stiffness, the elastic modulus $E_{50}$ was determined as the slope of the deviatoric stress–axial strain plot corresponding to 50% of the maximum deviatoric stress that the samples reached before failure.

Figure 12 shows the relationship between $E_{50}$, water content and hydraulic paths for samples subjected to 1 and 6 cycles while the suction values are shown as labels of the data points. The results indicated a general reduction in $E_{50}$ with an increase in the water content and the hydraulic cycles. The wetted samples showed lower $E_{50}$ values compared to the dried samples at the same hydraulic cycle due to the lower suction and more ductile behaviour of the samples under wetting conditions (Wheeler et al. 2003; Khoury and Zaman 2004). $E_{50}$ also decreased when samples were subjected to a higher number of hydraulic cycles. However, when comparing the results of 1st and 6th cycles, the suction level is not exclusively explaining the changes in $E_{50}$. For example, 6D with $s$ of 3.86 MPa (or 6W with $s$ of 4.05 MPa) exhibited lower $E_{50}$ than 1D with $s$ of 3.61 MPa (or 1W with $s$ of 2.99 MPa).

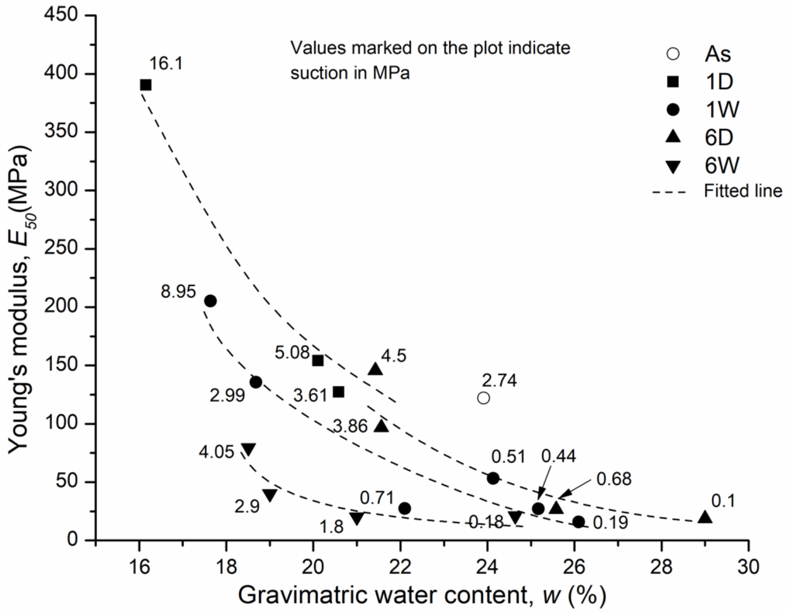


Fig 12. The elastic modulus $E_{50}$ with respect to water content and the hydraulic paths

## 5.0 DISCUSSION

Figure 13a shows the peak deviatoric stress $q_p$ for samples upon various hydraulic paths with their suction values indicated as labels of the data points. The strength increased from As to 1D due to the increase in suction while the suction loss due to the water retention hysteresis reduced $q_p$ of 1W. Sample 3D, having a water content similar to 1D, exhibited a lower $q_p$ due to the suction loss resulting from shifts in the drying water retention capacity. On the other hand, 3D and 3W exhibited a peak strength similar to that of 1W as all these three samples have a similar suction of around 3 MPa. In contrast, 6D and 6W, which had a higher suction level than 1W, 3D and 3W, showed a noticeable reduction in $q_p$.

Figure 13b shows $q_p$ for all tested samples with respect to suction where suction values are plotted on the logarithmic scale to emphasise the effect of cracking on the shear strength of the soil. The results indicate that $q_p$ of the samples subjected to 1 and 3 cycles was primarily governed by the suction level with $q_p$ increasing as the suction level rises. However, $q_p$ of the samples subjected to 6 cycles clearly lie below the envelop in which the suction dependent strength behaviour was observed. A curve projecting the variation of $q_p$ for the samples subjected to 6 drying and wetting cycles indicated a distinct reduction of about 40% when compared to the average curve projected for the data within the envelope. Using the logarithmic scale to present the suction data enhances the clarity of how drying-wetting cycles impact soil strength, particularly within the suction range below 6 MPa where data exhibit scattering. However, it is important to acknowledge that the logarithmic scale may exaggerate the apparent rate of the strength increase.

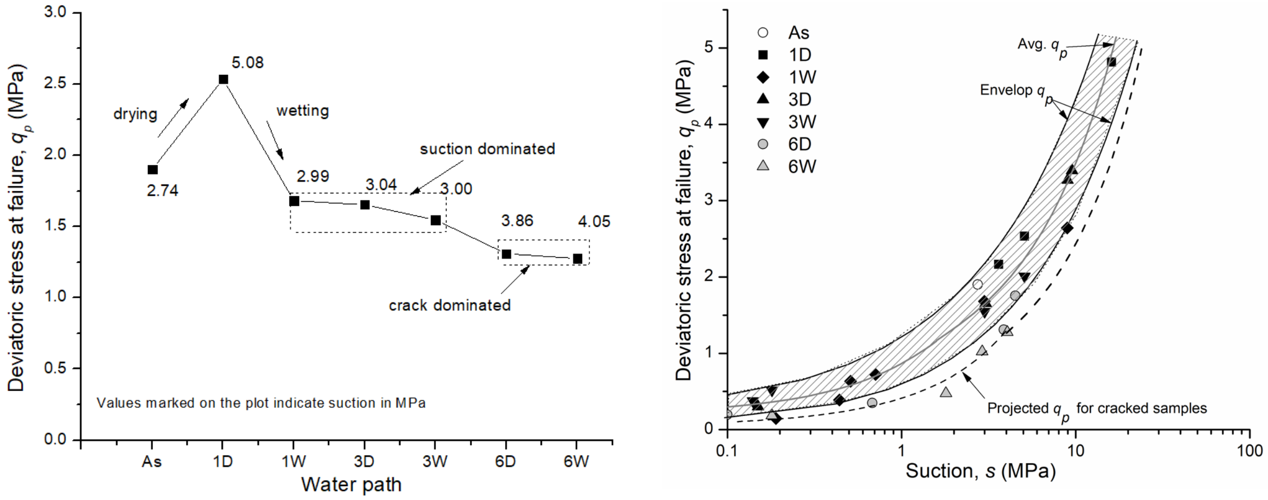


(a) (b)

Fig 13. The relationship between the deviatoric stress at failure and (a) water paths (b) suction levels

The results suggest the initial drying and wetting cycles (up to 3 cycles) reduce the water retention capacity and cause suction losses due to microstructural changes and development of microcracks within the soil. Despite these changes, the shear strength of the soil mass remains predominantly dependent on suction over the initial cycles regardless of the hydraulic path followed. During the following cycles, further development and propagation of prominent cracks degraded the soil and eventually brings the strength to a lower level compared to the soil strength measured during the initial cycles. This is consistent with the change in compaction characteristics of the soil with successive cycles as discussed earlier, i.e. the density reduces after 6 cycles.

The strength characteristics of the tested soil are also interpreted using Bishop′s stress (Bishop 1959). Normal Bishop′s stress $\sigma^*$ is defined as $\sigma^* = \frac{\sigma_1+\sigma_3}{2} + S_r s$, where $\sigma_1$ and $\sigma_3$ are the net axial and radial stresses, respectively, $S_r$ is the degree of saturation and $s$ is the suction. $S_r$ is used in place of Bishop′s parameter as it describes the average stress acting on the soil skeleton (Jommi 2000) where $S_r s$ incorporates the effect of suction bonding present in unsaturated soils (Wheeler et al. 2003). The measurement of $S_r$ was not possible for all samples at the end of the tests as the samples with higher suction values crumbled during shearing rather than showing a progressive failure. Therefore, $S_r$ used for interpretation was measured based on the initial density of the samples before shearing, assuming it would remain constant during shearing as the volume change of the samples with very high suction levels was very small under the constant water content condition.

Figure 14a shows the failure envelopes fitted to the data points, represented in terms of peak shear strength $\tau_p = \frac{\sigma_1 - \sigma_3}{2}$ and normal Bishop′s stress $\sigma^*$ for all samples, including those subjected to 1st (1D/W), 3rd (3D/W) and 6th (6D/W) cycles. The result indicates changes in the failure envelop (particularly at $\sigma^*$ < 4 MPa) with drying and wetting cycles where the peak strength reduced from 1st to 3rd cycles and then from 3rd to 6th cycles. The progressive degradation of the soil strength with drying and wetting cycles can be recognised, even during the initial cycles, when both suction and degree of saturation are considered for the interpretation of the shear behaviour of the tested soil. This could imply that the effect of the initial hydraulic cycles on the strength of the soil was not detectable, partially due to the varying degree of saturation among the data points. But it has to be pointed out that the shear strength data points show some scatter when plotted against Bishop′s stress which makes drawing such conclusions tentative.

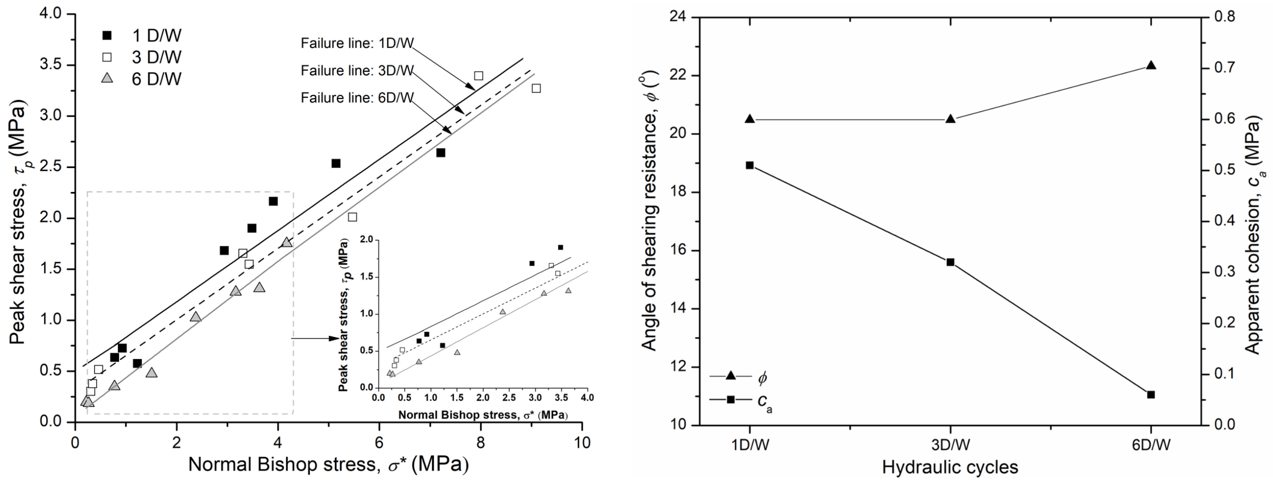


(a) (b)

Fig 14. (a) Peak shear strength $\tau_p$ and normal Bishop's stress $\sigma^*$
(b) Changes in apparent cohesion $c_a$ and friction angle $\varphi$ with hydraulic cycles

Figure 14b shows the evolution of shear strength parameters (the apparent cohesion $c_a$ and the angle of shearing resistance $\varphi$ based on $\tau_p = c_a + \sigma^* \tan\varphi$) with hydraulic cycles. It can be observed that $c_a$ reduced from 0.51 MPa to 0.06 MPa (80% reduction) from 1st to 6th cycles while changes in $\varphi$ with drying and wetting cycles were insignificant. This suggests that the development and propagation of desiccation cracking during drying and wetting cycles mainly contributed to the deterioration of the inter-particle or inter-aggregate bonding within the soil, leading to a reduction of the apparent soil cohesion. On the other hand, the angle of shearing resistance remained relatively unchanged because the particle-to-particle or aggregate-to-aggregate friction was not significantly influenced by the development of the cracks during drying and wetting cycles.

To further explore the shear strength behaviour of the tested soils, the results were also interpreted in terms of the microstructural based effective stress proposed by Alonso et al. (2010) for modelling the behaviour of unsaturated soils. The normal microstructural Bishop's stress $\sigma_M{}^*$ is defined as $\sigma_M{}^* = \frac{\sigma_1+\sigma_3}{2} + S_r{}^k s$, where $S_r{}^k$

represents the macroscopic degree of saturation. ${S_r}^k$ is used in place of Bishop′s parameter assuming that the capillary effect, governing the mechanical behaviour of soils, is present due to water occupying macropores rather than water within aggregates. $k$ regulates the fraction of the total degree of saturation that is attributed to macropores. $k$ was independently calibrated to find the best fit for samples subjected to the 1st, 3rd, and 6th cycles.

Figure 15a shows the peak shear strength $\tau_p$ against to the normal microstructural Bishop's stress ${\sigma_M}^*$ for all samples. The peak shear strength values show less scatter in relation to ${\sigma_M}^*$ when compared to their scatter against normal Bishop′s stress $\sigma^*$ (Figure 13a). This is particularly noticeable for $\sigma^*$ < 4 MPa where the $\tau_p$ values of 6D/W samples align with the $\tau_p$ values of 3D/W and 1D/W samples. As a result, a single failure line can be well-fitted to the data points in the case of ${\sigma_M}^*$ ($c_a = 0.16$ MPa and $\varphi = 17°$).

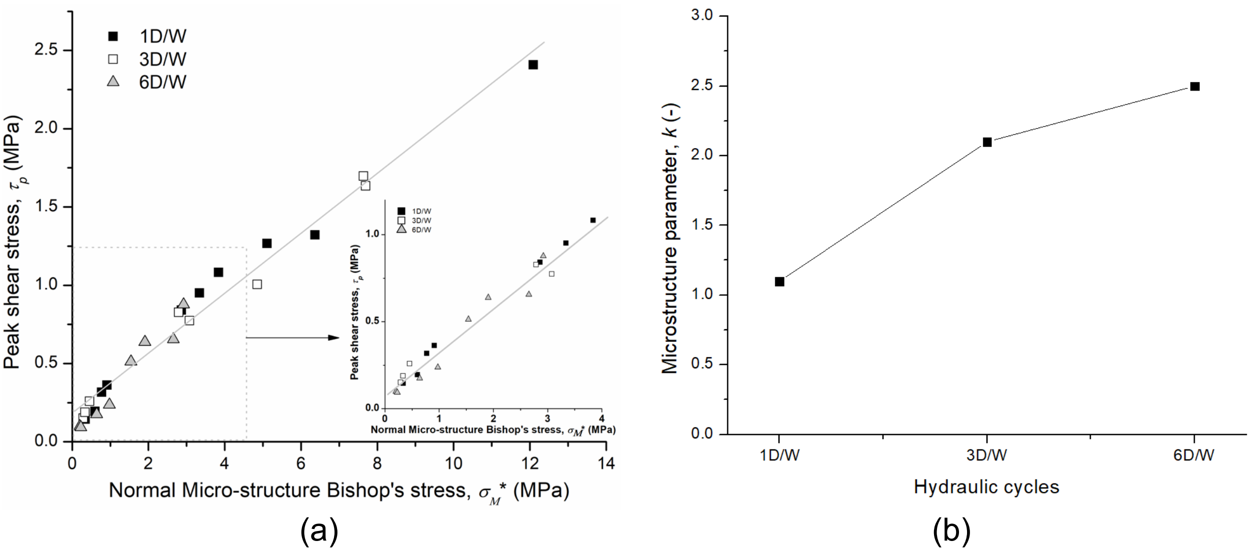


(a) (b)

Fig 15. (a) Peak shear strength $\tau_p$ and normal microstructural stress ${\sigma_M}^*$
(b) Changes in the parameter $k$ with hydraulic cycles

Figure 15b shows the values of the parameter $k$ used for samples subjected to different hydraulic cycles where $k$ increases with successive drying – wetting cycles. The increase in $k$ from 1.1 to 2.5 indicate a reduction in ${S_r}^k$, and in turn, a decrease in the degree of saturation of macropores. This is consistent with the increase in the volume of large pores within the soil due to the development of microcracks and surficial cracks during drying and wetting cycles. $k = 1.1$ for the samples subjected to the 1st drying and wetting cycle means ${\sigma_M}^*$ is similar to Bishop′s stress $\sigma^*$ (${S_r}^k \approx S_r$). This aligns with the proposition put forth by Alonso et al. (2010), which suggests that for very clayey soils with aggregated structures, similar to the soil tested in this study, using $S_r$ as Bishop′s parameter is more suitable than ${S_r}^k$. However, $k$ around 1 does not seem to reproduce the shear strength data of the tested soils when subjected to further drying – wetting cycles. As crack development increases the volume of large pores within the soil mass and lowers the macroscopic degree of saturation, the contribution of the total degree of saturation requires reductions through an increase in $k$ to 2.1 and 2.5 with 3 and 6 cycles, respectively.

The results showed the successive drying-wetting cycles led to suction losses associated with the shifts and reductions in the water retention capacity of the tested soil, alongside hysteresis effects. However, the changes in the shear strength of the soil could not be solely attributed to these suction losses, as the development of desiccation cracks also altered the fundamental properties of the soil. Nevertheless, the degradation effect of crack development on the shear strength of the tested soil, subjected to hydraulic cycles, was found to be explained by the contribution of the degree of saturation rather than the cracking mechanism. The effect on the shear strength was justified by employing the macroscopic degree of saturation through the microstructural-based effective stress, providing that *k* values change with drying and wetting cycles. This accounted for the increase in the size of large pores due to crack development. Despite the presence of cracks from hydraulic cycles, the high level of suction in the soil and the capillary effect present within the pores also influence the mechanical behaviour of the soil.

A similar trend was also observed in the stiffness behaviour of the tested soil. Figure 16a shows the elastic modulus $E_{50}$ against suction. Plotting suction values on a logarithmic scale helps to highlight the effects of drying-wetting cycles and cracks on the stiffness at suction levels below 6 MPa, which is not clearly visible on a linear scale due to the wide range of suction values involved. $E_{50}$ was dependent on suction but also decreased from the 1st to 3rd and 6th cycles regardless of the suction levels. This implies that the development of microcracks during initial cycles affect the stiffness of the tested soil as well as surficial cracks observed along the following cycles. When $E_{50}$ values were plotted against the normal microstructural stress $\sigma_M{}^*$ (Figure 16b), a good correlation was observed between the two data sets. Interestingly, the same values obtained for $k$ to analyse the shear strengths effectively captured the stiffness values for the samples subjected to 1st cycle ($k$ = 1.1), 3rd cycle ($k$ = 2.1) and 6th cycle ($k$ = 2.5), implying that progressive microstructural changes during the applied drying and wetting cycles continuously affected the stiffness behaviour of the soil.

Various microstructural-based approaches have been proposed to explain the hydro-mechanical behaviour of unsaturated soils, such as those by Gens and Alonso (1992), Alonso et al. (2010), Della Vecchia et al. (2013) and Musso et al. (2020). In the present study, it was found that the contribution of the microstructural aspect (in this case the macroscopic degree of saturation) evolved with drying and wetting cycles, requiring the establishment of a relationship between the microstructural framework and hydraulic cycles.

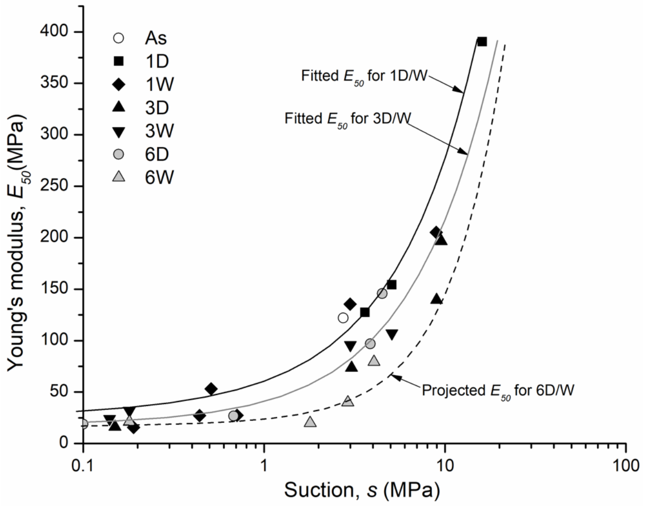


(a)

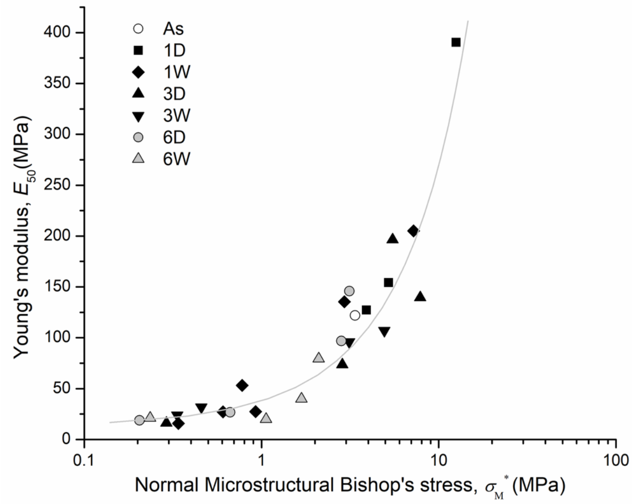


(b)

Fig 16. The elastic modulus *E₅₀* with respect to (a) suction (b) normal microstructural stress $\sigma_M{}^*$

## 6.0 CONCLUSION

The work described in this paper provides insights into the effects of drying and wetting cycles and desiccation cracks on the soil water retention properties, shear strength and elastic modulus of a compacted clayey soil taken from a road subgrade layer in Tanzania. The improvement in the understanding of these mechanisms will help in predicting the long-term performance of the compacted soils used in linear infrastructure under weather-driven water fluctuation due to climate changes.

The experimental campaign included performing cyclic drying-wetting, water retention testing and stress-strain shearing on the samples subjected to 1$^{st}$, 3$^{rd}$ and 6$^{th}$ cycles of drying and wetting. The results showed reductions in the water retention capacity of the soil accompanied by subsequent shifts in the water retention curves with successive drying and wetting cycles. This also affected the stress-strain response of the soil to shear loading where the shear strength and elastic modulus of the soil subsequently reduced from 1$^{st}$ to 3$^{rd}$ and 6$^{th}$ cycles. While the soil experienced suction losses due to shifts and reductions in its water retention capacity, resulting from the development and propagation of desiccation cracks and the hysteresis effect between drying and wetting, these suction losses were not solely responsible for the observed changes in shear strength. For instance, certain samples subjected to $6^{th}$ drying-wetting cycles exhibited lower shear strength values than samples subjected to a lower number of cycles, despite having higher suction levels. The development of desiccation cracks played a significant role in altering the fundamental properties of the soil and contributed to the deterioration of its strength and stiffness.

Nonetheless, the study revealed that the degradation effect of crack development on the shear strength and elastic modulus for the soil tested in this study, under the influence of hydraulic cycles, could be explained by considering the contribution of the degree of saturation rather than the cracking mechanism. This was supported by employing a fraction of the total degree of saturation attributed to the macrostructural pores (those external to the aggregates within the soil) through a microstructural-based effective stress approach. This allowed accounting for the reduced contribution of the total degree of saturation to the generation of strength, attributed to the enlargement of large pores resulting from the development of cracks. With the microstructural-based effective stress approach, the successive changes in shear strength and stiffness with drying and wetting cycles observed in the soil could be effectively explained and justified.

In conclusion, the repetitive drying and wetting cycles have a profound impact on both the hydraulic and mechanical properties of compacted soils, due to the fabric changes as well as development of desiccation cracks. These deterioration effects on soil characteristics can significantly influence the long-term performance of geotechnical structures constructed with such soils, particularly in regions prone to extreme weather events or situated near water bodies. Therefore, it becomes imperative to consider the effects of hydraulic cycles during the design of geotechnical infrastructure to ensure the reliability and stability of infrastructure projects.


## ACKNOWLEDGEMENT

The authors would like to acknowledge the funding received from UK Engineering and Physical Sciences Research Council (EPSRC) through Global Challenges Research Fund (GCRF) to carry out the research titled 'Sustainability and resilience of transportation infrastructure in African countries' grant number - EP/P029671/1.


## Competing Interests Statement

The authors declare that they have no known competing financial interests or personal relationships that could have appeared to influence the work reported in this paper.

## Data Availability Statement

Data that support the findings of this study are available from the corresponding author upon reasonable request.

## REFERENCES


Airò Farulla, C., Ferrari, A., and Romero, E. (2010). Volume change behaviour of a compacted scaly clay during cyclic suction changes. *Canadian Geotechnical Journal*, 47(6): 688–703. doi:10.1139/T09-138.

Albrecht, B. and Benson, C. (2001). Effect of desiccation on compacted natural clays. *Journal of Geotechnical and Geoenvironmental Engineering*, 127(1): 67–76. doi:10.1061/(ASCE)1090-0241(2001)127:1(67)

Alonso E.E., Pereira J. M., Vaunat J. and Olivella S. (2010). A microstructurally based effective stress for unsaturated soils. *Géotechnique* 60:12, 913-925

ASTM D6836-02, (2002). Standard test methods for determination of the soil water characteristic curve for desorption using hanging column, pressure extractor, chilled mirror hygrometer, or centrifuge. Annual Book of ASTM Standards. West Conshohocken, PA: ASTM International.

Azizi, A., Kumar, A., Lingwanda, M. I., and Toll, D. G. (2020a). The influence of rates of drying and wetting on measurements of soil water retention curves. E3S Web of Conferences, 195, 03005. https://doi.org/10.1051/e3sconf/202019503005

Azizi, A., Kumar, A. and Toll. D. G. (2023a). Coupling cyclic and water retention response of a clayey sand subjected to traffic and environmental loading cycles. *Géotechnique* 73 (5), 401-417 https://doi.org/10.1680/jgeot.21.00063.

Azizi, A., Kumar, A. and Toll, D. G., (2023b). The bounding effect of the water retention curve on the cyclic response of an unsaturated soil. *Acta Geotechnica*. https://doi.org/10.1007/s11440-022-01724-0

Azizi A., Musso, G. and Jommi C. (2020b). Effects of repeated hydraulic loads on microstructure and hydraulic behaviour of a compacted clayey silt. *Can. Geotech. J.* 57(1): 100-114.

Azizi, A., Musso, G., Jommi, C. and Cosentini, R. M. (2018). Evolving fabric and its impact on the shearing behaviour of a compacted clayey silt exposed to drying-wetting cycles. In *Proceedings of the 7th International Conference on Unsaturated Soils (UNSAT2018)*, Hong Kong, pp. 641–646.

Bishop, A. W. (1959). The principle of effective stress. *Tecknisk Ukeblad* 106, No. 39, 859–863.

Briggs K. M., Helm P. R., Smethurst J. A., Smith A., Stirling R., Svalova A., González Y. T., Loveridge F. A. and Glendinning S. (2023). Evidence for the weather-driven deterioration of ageing transportation earthworks in the UK. *Transportation Geotechnics*, 43: 101130. https://doi.org/10.1016/j.trgeo.2023.101130.

BSI (1990). BS 1377: Part 2: Classification tests. London, UK: British Standards Institution.

BSI (1990). BS 1377: Part 4: Compaction tests. London, UK: British Standards Institution.

Cui, Y. J., Loiseau, C. and Delage, P. (2002). Microstructure changes of a confined swelling soil due to suction controlled hydration. *Proceeding of 3rd Int. Conf. on Unsaturated Soils (UNSAT 2002)*, Recife, Brazil (ed. Jucá, J. F. T., de Campos, T. M .P. and Marinho, F .A .M.), Lisse: Swets and Zeitlinger, Vol. 2, pp. 593-598.

Chinowsky, P., Schweikert, A., Strzepek, N., Manahan, K., Strzepek, K., and Schlosser, C.A. (2013). Climate change adaptation advantage for African road infrastructure. *Climatic Change*, 117(1) pp. 345–361.

Dias A S., Hughes, P.N., Toll, D.G. and Glendinning, S. A simple method to determine soil-water retention curves of compacted active clays, *Transportation Geotechnics,* 43: 101138.

Della Vecchia, G., Jommi, C., and Romero, E. (2013). A fully coupled elastic–plastic hydromechanical model for compacted soils accounting for clay activity. *International Journal for Numerical and Analytical Methods in Geomechanics*, 37: 503–535. doi:10.1002/nag.1116.

Fredlund, G. D., Bergan, A. T., and Sauer, E. K. (1975). "The deformation characteristics of subgrade soils for highways and runways in northern environments." *Can. Geotech. J.*, 12(2), 213–223.

Fredlund, D.G. and Rahardjo, H. (1993). Soil Mechanics for Unsaturated Soils. Wiley, New York.

Fredlund, D. G. and Xing, A. (1994). Equations for the soil-water characteristic curve. *Canadian Geotechnical Journal*, 31(4): 521–532.

Gallipoli, D., Gens, A., Sharma, R. and Vaunat, J. (2003). An elasto-plastic model for unsaturated soil incorporating the effects of suction and degree of saturation on mechanical behaviour. *Géotechnique* 53 (1): 123–135.

Gens, A., and Alonso, E.E. 1992. A framework for the behaviour of unsaturated expansive clays. *Canadian Geotechnical Journal*, 29: 1013–1032.

Goh, S. G., Rahardjo, H. and Leong, E. C. (2014). Shear strength of unsaturated soils under multiple drying-wetting cycles. *J. Geotech. Geoenviron. Engng* 140(2): 06013001.

Hen-Jones, R. M., Hughes, P. N., Stirling, R. A., Glendinning, S., Chambers, J. E., Gunn, D. A., and Cui, Y. J. (2017). Seasonal effects on geophysical–geotechnical relationships and their implications for electrical resistivity tomography monitoring of slopes. *Acta Geotch.* 12(5): 1159–1173.

Hillel, D. (1998). Environmental soil physics. Elsevier Science.

Jommi, C. (2000). Remarks on the constitutive modelling of unsaturated soils. In *Experimental evidence and theoretical approaches in unsaturated soils* (eds A. Tarantino and C. Mancuso), pp. 139–153. Rotterdam, the Netherlands: Balkema (Taylor & Francis Group).

Kumar, A., Azizi, A. and Toll D.G. (2022). The application of suction monitoring for cyclic triaxial testing of compacted soils. *J. Geotech. Geoenviron. Engng* 148(4): 04022009: 1-17.

Khoury, N. N., and Zaman, M. M. (2004). Correlation between resilient modulus, moisture variation, and soil suction for subgrade soils. Transportation research record, 1874(1), 99-107.

Li, ZS., Korkiala-Tanttu, L. and Sołowski, W. (2023). Measurement of three-dimensional shrinkage deformations and volumes of stabilised soft clay during drying with Structure from Motion photogrammetry. *Acta Geotechnica* 18, 5319–5339.

Lloret, A., Villar, M.V., S.nchez, M., Gens, A., Pintado, X., and Alonso, E.E. (2003). Mechanical behaviour of heavily compacted bentonite under high suction changes. *Géotechnique*, 53(1): 27–40. doi:10.1680/geot.2003.53.1.27.

Lu, N., and Kaya, M. (2014). Power Law for Elastic Moduli of Unsaturated Soil. *Journal of Geotechnical and Geoenvironmental Engineering*, 140(1), 46–56.

METER Group I. WP4C Dew Point PotentiaMeter Operator’s Manual. 2018.

Mendes, J. and Toll, D. G. (2016). Influence of Initial Water Content on the Mechanical Behavior of Unsaturated Sandy Clay Soil. *International Journal of Geomechanics* 16(6): 1–18.

Mu, Q. Y., Dong, H., Liao, H. J., Dang, Y. J. and Zhou, C. (2020). Water-retention curves of loess under wetting-drying cycles. *Geotechnique Letters* 10(2): 1–6.

Musso G, Azizi A and Jommi C (2020). A microstructure-based elastoplastic model to describe the behaviour of a compacted clayey silt in isotropic and triaxial compression. *Can Geotech J.* 57(7):1025–1043

Ng, C. W., and Pang, Y. W. (2000). Experimental investigations of the soil-water characteristics of a volcanic soil. Canadian Geotechnical Journal, 37(6), 1252-1264.

Ng, C. W. W., Xu, J., and Yung, S. Y. (2009). Effects of imbibition- drainage and stress ratio on anisotropic stiffness of an unsaturated soil at very small strains. *Can. Geotech. J.*, 46(9), 1062–1076.

Nowamooz, H. and Masrouri, F. (2009). Density-dependent hydromechanical behaviour of a compacted expansive soil. *Engng Geol.* 106: 105–115.

Pasha A. Y., A. Khoshghalb, and N. Khalili, (2016). Pitfalls in Interpretation of Gravimetric Water Content–Based Soil-Water Characteristic Curve for Deformable Porous Media. *International Journal of Geomechanics*: 16(6) D4015004.

Romero, E., Vecchia, G.D. and Jommi, C. (2011). An insight into the water retention properties of compacted clayey soils. *Géotechnique* 61(4): 313-328.

Rouainia, M., Helm, P., Davies, O., and Glendinning, S. (2020). Deterioration of an infrastructure cutting subjected to climate change. *Acta Geotechnica*, 15(10), 2997-3016. doi: 10.1007/s11440-020-00965-1

Stirling, R.A., Toll, D.G., Glendinning, S., Helm, P.R., Yildiz, A., Hughes, P.N. and Asquith, J.D. (2021). Weather-driven deterioration processes affecting the performance of embankment slopes. *Géotechnique* 71(11): 957-969.

Tang, A. M., Vu, M. N., and Cui, Y. J. (2011). Effects of the maximum soil aggregates size and cyclic wetting-drying on the stiffness of a lime-treated clayey soil. *Géotechnique* 61(5): 421–429.

Tang, C. S., Cheng, Q., Leng, T., Shi, B., Zeng, H., and Inyang, H. I. (2020). Effects of wetting-drying cycles and desiccation cracks on mechanical behavior of an unsaturated soil. *Catena*, 194, 104721.

Tarantino, A. (2009). A water retention model for deformable soils. *Géotechnique*, 59(9), 751–762

Toll, D. G. (2015). California Bearing Ratio tests on a lateritic gravel from Kenya. *Transportation Geotechnics*, 5, 59–67.

Toll, D. G. (1990). A framework for unsaturated soil behaviour. *Geotechnique* 40(1): 31–44.

van Genuchten, M. T. (1980). A closed-form equation for predicting the hydraulic conductivity of unsaturated soils. *Soil Sci. Soc. Am. J.* 44(5): 892–898.

Wen, T., Shao, L., and Guo, X. (2021). Effect of hysteresis on hydraulic properties of soils under multiple drying and wetting cycles. European Journal of Environmental and Civil Engineering, 25(10), 1750-1762.

Wheeler S. (1996). Inclusion of specific water volume within an elastoplastic model for unsaturated soils. *Canadian Geotechnical Journal*, 33:42–57. 5.1

Wheeler, S. J., Sharma, R. S. and Buisson, M. S. R. (2003). Coupling of hydraulic hysteresis and stress–strain behaviour in unsaturated soils. *Géotechnique* 53, No. 1, 41–54, https://doi.org/10.1680/geot.2003.53.1.41.

Xu, J., Zhang, H., Tang, C., Cheng, Q., Liu, B. and Shi, B. (2022). Automatic soil desiccation crack recognition using deep learning. *Géotechnique*, 72(4): 337-349.

Xu, X., Shao, L., Huang, J., Xu, X., Liu, D., Xian, Z. and Jian, W. (2021). Effect of wet-dry cycles on shear strength of residual soil. *Soils and Found.* 61(3): 782–797.

Yu, Z., Eminue, O.O., Stirling, R., Davie, C. and Glendinning, S., (2021). Desiccation cracking at field scale on a vegetated infrastructure embankment. *Géotechnique Letters* 11(1):1-21.

Zuo, C., Liu, D., Ding, S. and Chen, J. (2016) Micro-characteristics of strength reduction of tuff residual soil with different moisture," *KSCE J Civil Engng.*, 20(2), 639-646.

LIST OF FIGURES

Fig 16. The elastic modulus $E_{50}$ with respect to (a) suction (b) normal microstructural stress $\sigma_M{}^*$

LIST OF TABLES

Table 1. Properties of soil sample under the constant water content condition

| Sample No. | Dry Density, $\rho_d$ ($Mg/m^3$) | Water content, $w$ (%) | Suction, $s$ (MPa) | Sample Type |
|---|---|---|---|---|
| Drying-wetting sample | | | | |
| 1 | 1.54 | 23.5 | - | As |
| 2 | 1.55 | 23.5 | - | As |
| Soil-water retention testing sample | | | | |
| 1 | 1.55 | 24.2 | 0.4 | As |
| 2 | 1.51 | 25.9 | 0.6 | 3D |
| 3 | 1.51 | 24.4 | 0.44 | 6D |
| 4 | 1.69 | 4.0 | 128 | 1D |
| 5 | 1.66 | 2.98 | 129 | 3W |
| 6 | 1.68 | 2.5 | 132 | 6W |
| Constant water content samples | | | | |
| 1 | 1.54 | 23.9 | 2.74 | As |
| 2 | 1.56 | 20.6 | 3.61 | 1D* |
| 3 | 1.57 | 20.1 | 5.08 | 1D |
| 4 | 1.58 | 16.2 | 16.1 | 1D |
| 5 | 1.51 | 25.1 | 0.44 | 1W* |
| 6 | 1.50 | 26.1 | 0.19 | 1W |
| 7 | 1.55 | 17.6 | 8.95 | 1W |
| 8 | 1.55 | 18.7 | 2.99 | 1W |
| 9 | 1.50 | 22.1 | 0.71 | 1W |
| 10 | 1.52 | 24.1 | 0.51 | 1W |
| 11 | 1.52 | 24.6 | 0.04 | 3D* |
| 12 | 1.55 | 21.7 | 3.04 | 3D |
| 13 | 1.61 | 20.3 | 8.15 | 3D |
| 14 | 1.60 | 16.3 | 9.53 | 3D |
| 15 | 1.59 | 22.1 | 5.09 | 3W* |
| 16 | 1.56 | 23.3 | 3.00 | 3W |
| 17 | 1.57 | 25.7 | 0.18 | 3W |
| 18 | 1.50 | 27.1 | 0.14 | 3W |
| 19 | 1.44 | 30.2 | 0.07 | 6D* |
| 20 | 1.47 | 25.6 | 0.68 | 6D |
| 21 | 1.52 | 21.6 | 3.86 | 6D |

| | | | | |
|---|---|---|---|---|
| 22 | 1.49 | 21.4 | 4.50 | 6D |
| 23 | 1.48 | 24.6 | 0.18 | 6W* |
| 24 | 1.47 | 21.0 | 1.80 | 6W |
| 25 | 1.48 | 19.5 | 3.90 | 6W |
| 26 | 1.48 | 18.5 | 4.05 | 6W |

* 'As' indicates as-compacted state of the sample and '1*D*' indicates the sample being air-dried from the 'As' state. '1W" indicate the 1st cycle of wetting (after the 1st air-drying), '3D' indicates the sample subjected to the 3rd drying path (following the second drying-wetting cycle), '3W' indicates the sample subjected to 3 cycles of drying and wetting. Similarly, '6D' indicates the sample is subjected to 6 drying cycles following 5 drying-wetting cycles and '6W' indicates the sample is subjected to 6 full cycles of drying and wetting.

Table 2. Parameters of the water retention model

| Hydraulic path | vG model parameters | | water content parameters | |
|---|---|---|---|---|
| | $\alpha$ | $n$ | $w_s$ | $w_r$ |
| Drying: 1*D*, 3*D*, 6*D* | 0.05, 0.08,0.10 | 1.92,1.69,1.65 | 24.5, 26.5, 25 | 1.6 |
| Wetting: 1*W*, 3*W*, 6*W* | 0.10, 0.13, 0.14 | 1.64,1.69,1.65 | 24.5, 25, 24.5 | 1.6 |